Role of P-Glycoprotein and the Intestine in the Excretion of DPC 333 [(2R)-2-{(3R)-3-Amino-3-[4-(2-methylquinolin-4-ylmethoxy)phenyl]-2-oxopyrrolidin-1-yl}-N-hydroxy-4-methylpentanamide] in Rodents

C. Edwin Garner, Eric Solon, Chii-Ming Lai, Jianrong Lin, Gang Luo, Kevin Jones,
Jingwu Duan, Carl P. Decicco, Thomas Maduskuie, Stephen E. Mercer, Lian-Shen Gan,
Mingxin Qian, Shimoga Prakash, Huey-Shin Shen, and Frank W. Lee

Infection and Cancer Discovery, AstraZeneca PLC, Waltham, Massachusetts (C.E.G.).; Preclinical Development Drug Metabolism and Pharmacokinetics, AstraZeneca Plc, Wilmington, Delaware (J.L.); Infection and Cancer Discovery, AstraZeneca Plc, Macclesfield, United Kingdom (K.J.); Quest Pharmaceutical Services Inc, Newark, Delaware (E.S., C.-M.L., H.-S.S.); Bristol-Myers Squibb Company, Pennington, New Jersey (G.L., J.D., C.P.D., S.E.M., S.P.); Boehringer Ingelheim Pharmaceuticals, Ridgefield, Connecticut (L.-S.G.); Pharmacokinetics, Pharmacodynamics and Bioanalytical Sciences, Genentech Inc., San Francisco, California (M.Q.); Incyte Pharmaceuticals, Newark, Delaware (T.M.); and Millennium Pharmaceuticals, Inc., Cambridge, Massachusetts (F.W.L.)

ABSTRACT:

The role of the intestine in the elimination of (2R)-2-{(3R)-3-amino-3-[4-(2-methylquinolin-4-ylmethoxy)phenyl]-2-oxopyrrolidin-1-yl}-N-hydroxy-4-methylpentanamide (DPC 333), a potent inhibitor of tissue necrosis factor α–converting enzyme, was investigated in mice and rats in vivo and in vitro. In Madine-Darby canine kidney cells stably transfected with P-glycoprotein (P-gp) and DPC 333, the transport from B→A reservoirs exceeded the transport from A→B by approximately 7-fold. In Caco-2 monolayers and isolated rat ileal mucosa, DPC 333 was transported from basolateral to apical reservoirs in a concentration-dependent, saturable manner, and transport was blocked by N-(4-[2-(1,2,3,4-tetrahydro-6,7-dimethoxy-2-isoquinolinyl)ethyl]-phenyl)-9,10-dihydro-5-methoxy-9-oxo-4-acridine carboxamide (GF120918), confirming the contri- bution of P-gp/breast cancer resistance protein in B→A efflux of DPC 333. In quantitative whole body autoradiography studies with [14C]DPC 333 in mice and rats, radioactivity was distributed throughout the small intestine in both species. In GF120918-pretreated bile duct–cannulated rats, radioactivity in feces was reduced 60%. Using the in situ perfused rat intestine model, ~20% of an i.v. dose of [14C]DPC 333 was measured in the intestinal lumen within 3 h postdose, 12% as parent. Kinetic analysis of data suggested that excreted DPC 333 may be further metabolized in the gut. Intestinal clearance was 0.2 to 0.35 l/h/kg. The above data suggest that in the rodent the intestine serves as an organ of DPC 333 excretion, mediated in part by the transporter P-gp.

The literature contains evidence for direct intestinal secretion of a number of structurally diverse xenobiotics ranging from inorganic metals (Zalups, 1998) to large organic molecules such as digoxin (Caldwell et al., 1980). Evidence has accumulated to suggest that active intestinal secretion may play a major part in the elimination of several drugs (Mayer et al., 1996; Rabbaa et al., 1996; Sparrenboom et al., 1997; Smit et al., 1998a,b; Dautrey et al., 1999; van Asperen et al., 2000; Leusch et al., 2002; Li et al., 2005; Lagas et al., 2006; Villanueva et al., 2006).

P-glycoprotein (P-gp, MDR1) and breast cancer resistance protein (BCRP, ABCG2) are ATP-dependent multidrug efflux pumps belonging to the ATP-binding cassette superfamily of proteins (Hyde et al., 1990; Allen et al., 1999) that protect cells from xenobiotics by transporting them out of cells and reducing their intracellular levels. Physiologically, these transporters are widely expressed in the epithelial cells of intestine, liver, and kidney and in the endothelial cells of brain and placenta (Eisenblatter et al., 2003; Yeboah et al., 2006). The broad substrate specificity and distinctive expression locations suggest that P-gp/BCRP may have a direct role in modulating the absorption and disposition of drugs or xenobiotics (Hall et al., 1999; Merino et al., 2005; Zhang et al., 2005). The acridonecarboxamide derivative GF120918 potently inhibits both of these transporters

---

ABBREVIATIONS: P-gp, P-glycoprotein; MDR, multidrug resistance; BCRP, breast cancer resistance protein; GF120918, N-(4-[2-(1,2,3,4-tetrahydro-6,7-dimethoxy-2-isoquinolinyl)ethyl]-phenyl)-9,10-dihydro-5-methoxy-9-oxo-4-acridine carboxamide; DPC 333, (2R)-2-{(3R)-3-amino-3-[4-(2-methylquinolin-4-ylmethoxy)phenyl]-2-oxopyrrolidin-1-yl}-N-hydroxy-4-methylpentanamide; TEER, transepithelial electronical resistance; MDCK, Madine-Darby canine kidney; HPLC, high-performance liquid chromatography; QWBA, quantitative whole body autoradiography; IP, imaging plate; GI, gastrointestinal.
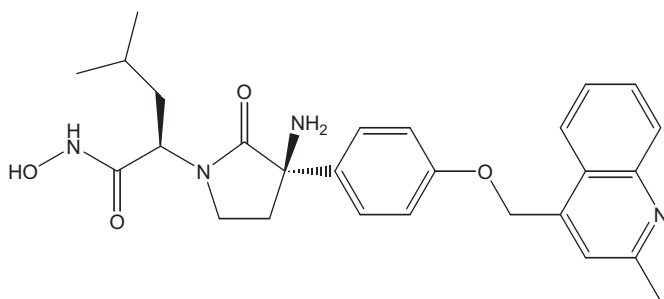
FIG. 1. Chemical structure of DPC 333.

(Hyafil et al., 1993; deBruin et al., 1999) and has been shown to be a useful research tool in investigations into the role of these transporters both in vivo and in vitro (Imbert et al., 2003; Breedveld et al., 2005; Hassan et al., 2006; Rautio et al., 2006).

Intestinal P-gp and/or BCRP may mediate the secretion of a large number of xenobiotics. Rabbaa et al. (1996) showed that the fluoroquinolone drug ofloxacin was actively cleared via the rat intestine and that this process was inhibited by other fluoroquinolones, including ciprofloxacin. Coadministration of the P-gp inhibitor verapamil reduced intestinal clearance by approximately 50%, suggesting a role of P-gp. Digoxin has also been shown to be actively secreted intestinally in rodents, and this process also was interrupted by known P-gp inhibitors (Mayer et al., 1996; Salphati and Benet, 1998). Transgenic mice, deficient in P-gp [mdr1(−/−)], have been used to show positively that intestinal excretion of a number of amphiphilic cationic drugs is mediated in part by P-gp (Sparreboom et al., 1997; Smit et al., 1998a,b; van Asperen et al., 2000; Lagas et al., 2006). Intestinal P-gp has also been suggested as a contributor to the clearance of digoxin, talinolol, and chemotherapeutic agents in humans (Greiner et al., 1999; Perdaems et al., 1999; Westphal et al., 2000). In elegant clinical experiments Westphal et al. (2000) showed in humans that induction of intestinal P-gp by rifampin correlated directly with an increase in the systemic clearance of i.v. administered talinolol in the absence of changes in metabolic clearance. Intestinal excretion of the food-derived heterocyclic amine carcinogen 2-amino-1-methyl-6-phenyl-imidazo[4,5-b]pyridine was shown to be markedly reduced in BCRP-deficient mice (van Herwaarden et al., 2003).

DPC 333 (Fig. 1) is a potent, orally active, selective inhibitor of tissue necrosis factor α–converting enzyme under evaluation for treatment of rheumatoid arthritis (Qian et al., 2007). To facilitate the clinical development of this compound, in vitro/in vivo disposition and excretion studies were conducted. Preliminary results of intestinal permeability screening studies performed in Caco-2 cell culture suggested that DPC 333 is a substrate for cellular efflux mechanisms, perhaps partly via the transporters P-gp or BCRP. The studies in this report were conducted to investigate the potential contribution of the intestine and the transporter P-gp to the elimination of DPC 333 in rodents in vivo.

Materials and Methods

In Vitro Transporter Studies. *ATPase activity assay.* In the present study, we expressed MDR1 in baculovirus-infected *Spodoptera frugiperda* ovarian insect cells and measured the ATP-dependent, vanadate-sensitive transport of known and potential MDR1 substrates using the method of Sarkadi et al. (1992). Briefly, a 60-μl reaction mixture containing 40 μg of membranes, 20 μM verapamil (positive control) or test drug, and 3 to 5 mM MgATP, 50 mM Tris-MES, pH 6.8, 2 mM EGTA, 50 mM KCl, 2 mM dithiothreitol, and 5 mM sodium azide was incubated at 37°C for 20 min. An identical reaction mixture containing 100 μM sodium orthovanadate was assayed in parallel. Orthovanadate inhibits P-gp by trapping MgADP in the nucleotide binding site. Thus,

ATPase activity measured in the presence of orthovanadate represents non–P-gp ATPase activity and can be subtracted from the activity generated without orthovanadate to yield vanadate-sensitive ATPase activity. The reaction was stopped by the addition of 30 μl of 10% SDS + antifoam A. Two additional reaction mixtures (+ and − orthovanadate but without MgATP) were also prepared and incubated with the others and then supplemented with SDS and MgATP to represent time = 0 min of reaction. The incubations were followed with addition of 200 μl of 35 mM ammonium molybdate in 15 mM zinc acetate/10% ascorbic acid (1:4) and incubated for an additional 20 min at 37°C. The liberation of inorganic phosphate was detected by its absorbance at 800 nm and quantitated by comparing the absorbance with a phosphate standard curve. The λ maximum for the measured phosphomolybdate chromophore is 850 nm; however, absorbance detection between 630 and 850 nm has been reported to be useful for this method (Drueke et al., 1990).

Caco-2 transport studies. Caco-2 cells were obtained from American Type Culture Collection (Manassas, VA). Cell stocks were maintained in T-75-cm^2 flasks (Costar, Corning, NY) at 37°C in a humidified atmosphere of 5% CO$_2$/95% air. The culture media consisted of high glucose (4.5 g/l) Dulbecco's modified Eagle's medium (GIBCO, Grand Island, NY) containing 10% fetal bovine serum (Hyclone, Logan, UT), 1% nonessential amino acids, 100 U/ml penicillin, and 100 mg/ml streptomycin (GIBCO). The culture media were replaced every other day. Monolayers were subcultured using 0.05% trypsin/0.02% EDTA when they reached 75 to 85% confluency at a split ratio of approximately 1:5.

Single-cell suspensions of Caco-2 cells were plated onto the 12-mm-diameter Transwell polycarbonate membranes (0.4-μm pore size, Costar) at a density of 6 × 10^4 cells/cm^2. The Transwell inserts were placed in 12-well culture plates with 0.5 ml of media in the apical compartment and 1.5 ml of media in the basolateral compartment. The media at both compartments were replaced every other day for 3 to 4 weeks before the cells were used for transport studies.

Before the transport experiments, the integrity of Caco-2 cell monolayers was assessed by determining transepithelial electronical resistance (TEER) using an Evon epithelial volt-ohm meter (World Precision Instruments, Inc., Sarasota, FL). TEER values were in the range of 400 to 800 Ω/cm^2. The culture medium in Transwell was aspirated and washed twice with transport buffer (Hanks' balanced salt solution containing 25 mM glucose and 10 mM HEPES, pH 7.4, except indicated). The cells then were incubated in the transport buffer at 37°C for 30 min. The transport was initiated by replacing transport buffer in the donor compartment with fresh transport buffer containing [^{14}C]DPC 333 with or without GF120918. After 2-h incubation, total radioactivity in media of receptor compartment was determined using Tri-Carb liquid scintillation analyzer (PerkinElmer Life and Analytical Sciences, Boston, MA).

Efflux in MDR1-transfected Madine-Darby canine kidney cells. Madine-Darby canine kidney (MDCK) II-MDR1 cells were obtained from The Netherlands Cancer Institute (Amsterdam, The Netherlands). Cell stocks were maintained in T-175-cm^2 flasks at 37°C in a humidified atmosphere of 5% CO$_2$/95% air. The culture media consisted of high glucose (4.5 g/l) Dulbecco's modified Eagle's medium containing 10% fetal bovine serum. The culture media were replaced every other day. Monolayers were subcultured using 0.05% trypsin/0.02% EDTA when they reached 75 to 85% confluency.

Single-cell suspensions of MDCKII-MDR1 cells were plated onto the 0.1-mm^2 Millicell-96 polycarbonate membranes (1-μm pore size, Millipore, Watford, UK) at a density of 4 × 10^5 cells/cm^2. The apical portion of the plate containing 150 μl of media was placed into the basolateral compartment containing 300 μl of media. The media were replaced 24 h before transport experiments.

Before transport experiments, the integrity of the MDCKII-MDR1 mono-layer was assessed by determining the TEER using the REMS TEER measurement system (WPI, Stevenage, UK). TEER values were in the range of 500 to 700 Ω/cm^2. The culture medium in the Millicell 96-well plates was aspirated and washed three times with transport buffer (Hanks' balanced salt solution containing 10 mM HEPES, pH 7.4). Transport was initiated by replacing transport buffer in the donor compartment with transport buffer containing DPC 333, verapamil, or vinblastine. For inhibition experiments, cyclosporin A was added to both apical and basolateral chambers. Following a 60-min

incubation period, aliquots were analyzed by liquid chromatography/tandem mass spectrometry.

Rat Intestinal Membrane Permeability Experiments. Sprague-Dawley rats were supplied by Charles River Canada Inc. (Senneville, QC, Canada). Ussing chambers and mounts were supplied by NaviCyte Co. (Reno, NV).

Male Sprague-Dawley rats (250 g) were anesthetized with ether, the abdomen opened, and the intestinal segments of interest were quickly removed and rinsed twice with chilled normal saline (0.9%). Smaller segments were cut (approximately 2.5 cm) and placed in cold Tyrode's buffer on ice, which was continuously bubbled with an O_2/CO_2 (95:5%) gas mixture. For these experiments ileal segments were used. Segments were cut along their mesenteric border, and the serosa was removed using blunt dissection. The mucosal side was rinsed with cold saline, and the segment was gently placed into position on the Ussing chambers (NaviCyte). During the preparation, the segments were submerged in Tyrode's buffer, which was bubbled continuously. The stripped intestinal mucosae from the rat ilium were then mounted in modified Ussing chambers with stirring conditions as described by Ungell et al. (1998). The effective exposed area of the tissues was 1.8 cm^2. All the experiments were carried out unidirectionally at 37°C. The serosal and the mucosal reservoirs were filled with Tyrode's buffer, and oxygen was provided to both chambers. To the donor compartment 5 ml of buffer containing test article (~0.3 μCi/ml) was added, and to the receiving compartment 5 ml of drug-free buffer was added. In parallel experiments, the potent P-gp/BCRP inhibitor GF120918 (0.2 μM) was added 10 min before the test article addition to determine the effect of P-gp/BCRP blockade on basolateral to apical transfer. Receiving chamber samples (0.2 ml) were removed at 15, 30, 45, 60, 75, 90, 105, and 120 min and replaced with equal amount of drug-free buffer. For the investigation of apical to basal transport, drug was placed in the mucosal side. For the investigation of basal to apical transport, drug was placed in the serosal side.

The radioactivity in each receiving chamber was determined by liquid scintillation spectrometry, and the cumulative radioactivity permeating the membrane was calculated. Analysis of representative medium samples for parent drug by high-performance liquid chromatography (HPLC) (see below) coupled with flow-through radiochemical detection showed stability under the experimental conditions above.

Quantitative Whole-Body Autoradiography Studies of [^{14}C]DPC 333 in Intact Mice and Bile Duct-Cannulated Rats. *Materials.* [^{14}C]DPC 333 was prepared by the Radiochemistry Department at DuPont Pharmaceuticals (Newark, DE). Specific activity was approximately 1 μCi/mg DPC 333. The radiolabeled dose, undiluted with cold material, was reconstituted on the day of dosing with sterile water for injection, USP.

Animals. Female BALB mice (approximately 25 g at study initiation) were obtained from Charles River Laboratories Inc. (Wilmington, MA). Male Sprague-Dawley rats, which were bile duct– and jugular vein–cannulated by the vendor, were obtained from Charles River Laboratories Inc.

Whole-body autoradiography. Animals were prepared for QWBA based on the methods of Ullberg (1954) as follows. Mice were individually housed with access to bottled water and were fasted overnight before dosing and during the in-life phase of the study. Each mouse received a single i.v. injection (tail vein) of 15 mg/kg (10 μCi/mouse). One mouse per time point was euthanized by carbon dioxide inhalation at 0.03, 0.25, 0.5, 1, 2, 4, 6, 12, and 24 h postdose. Each mouse carcass was frozen in a hexane/dry ice bath (approximately −70°C). Carcasses were then shipped to Quintiles, Inc. (Kansas City, MO) for processing, imaging, and quantitation of the amount of [^{14}C]DPC 333-derived radioactivity. Sections were exposed to phosphor imaging plates for 7 days and then scanned into an analytical imaging system workstation (Imaging Research, Inc., St. Catharine's, ON, Canada) via a GE Healthcare (Little Chalfont, Buckinghamshire, UK) phosphor image scanner. Glossy, black and white images of the autoradiographs were produced immediately after scanning. Annotated, composite images produced using the analytical imaging system were made to illustrate comparisons of tissue distribution. The lower limit of quantitation was determined by determining the lowest concentration of radioactivity in ^{14}C-spiked blood, which could be measured to an accuracy of < ±10% of the radioactivity concentration, which was determined by liquid scintillation spectroscopy and had an interimaging plate precision of <10%. This was determined for each imaging plate (IP) ($n = 10$, 1/rat) used for study as part of a system validation, which was performed before study initiation.

Three bile duct- and jugular vein-cannulated rats were administered a single i.v. dose of [^{14}C]DPC 333 (15 mg/kg, ~60 μCi/rat) via jugular vein cannula, and one rat each was euthanized by CO_2 inhalation at 2 and 5 min and at 1 h postdose. Rat carcasses were immediately frozen after death was confirmed by immersion in a hexane/dry ice bath. Carcasses were drained, blotted dry, and placed on dry ice for at least 2 h to complete the freezing process. Frozen rat carcasses were individually embedded along with section-thickness quality control standards (^{14}C-spiked rat blood) in carboxymethylcellulose (Chay and Poland, 1994) (frozen at approximately −70°C). Appropriate sections (~30 μm thick) were collected on adhesive tape (Nakagawa NA-70 MAG, Tokyo, Japan) using a Leica CM3600 cryomicrotome (Leica Microsystems, Deerfield, IL) with temperature controlled at approximately −20°C. Sections were collected at five levels of interest in the sagittal plane. All the major tissues, organs, and fluids were included in these levels. Sections were lyophilized, mounted on a black cardboard support along with ^{14}C-autoradiographic calibration standards (Code RPA 511, Amersham Life Sciences, Buckinghamshire, UK), wrapped with Mylar (DuPont) film, and exposed to phosphor IPs (BASIII, Fuji Photo Film Co., Ltd., Tokyo, Japan) for 4 days. Exposed IPs were scanned into the QWBA imaging system via an FLA 3000 BioImaging Analyzer (Fuji Biomedical Products, Fuji Photo Film Co., Ltd.), and digital images of the radioactivity in each section were obtained using M5+ MCID software (Imaging Research Inc.). Tissue concentrations were interpolated from each standard curve as nanocuries per gram and converted to microgram equivalents ^{14}C-labeled test article per gram of tissue. The concentrations of radioactivity in the calibration standards used ranged from 0 to approximately 9400 nCi/g tissue ($r^2 = 0.9994$–0.9999). Tissue concentrations were obtained from tissues that could be visually identified on the autoradiograph. The limit of quantitation was determined as the mean background radioactivity concentration value for background plus 3 times the S.D. (mean of 10 measurements/IP using sampling tools provided by the image analysis software, where small tool area = 1 × 1 mm; large sampling tool area = 5 × 5 mm). This was determined for small and large sampling tool areas on each IP ($n = 7$) used for study. Small tissues included the pituitary gland, adrenal gland, thyroid gland, skin, and bone marrow, and remaining tissues were considered as large tissues.

Disposition of [^{14}C]DPC 333 in Bile Duct-Cannulated Rats. *Materials.* Unlabeled DPC 333 was prepared by DuPont Pharmaceuticals. [^{14}C]DPC 333 was prepared by the Radiochemistry Department at DuPont Pharmaceuticals. Specific activity was approximately 4 μCi/mg DPC 333 free base. The radiolabeled dose, diluted with cold material, was reconstituted on the day of dosing with sterile water for injection, USP. GF120918 was prepared by the Radiochemistry Department at DuPont Pharmaceuticals. GF120918 doses were formulated in diethylene glycol/H_2O (1:9).

Animal mass balance studies. Male Sprague-Dawley rats (approximately 250 g at study initiation), fitted with indwelling bile duct cannulas for the collection of bile, were obtained from Charles River Laboratories Inc. Before administration of radiolabeled test compound, two rats were pretreated (20 mg/kg p.o.) with the potent P-gp and BCRP inhibitor GF120918 at 24 and 1 h predose. Each rat received a single i.v. injection (tail vein) of 15 mg/kg (5 ml/kg, 4 μCi/rat) of the dosing solution. Following administration of test material, each animal was placed into individual metabolism cages that allowed for separate collection of urine, feces, and bile. Bile was collected at 0.15, 0.5, 1, 2, 4, 8, 12, 24, 36, and 48 h postdose. Urine and feces were collected at 4, 12, 24, and 48 h postdose. At 48 h postdose, the animals were sacrificed by CO_2 asphyxiation, and the intestinal contents were collected into preweighed containers.

Sample analysis. Radioactivity in urine, cage washes, and bile was quantitated by directly assaying aliquots by liquid scintillation spectrometry. Total radioactive residues in solid samples (feces, intestinal contents) were determined by combusting aliquots of homogenized samples in an oxidizer (Packard Instruments, Meriden, CT), trapping the liberated [^{14}C]CO_2, and then analyzing samples by liquid scintillation spectrometry.

Samples were counted for 10 min or until 160,000 disintegrations (0.5% 2σ) were accumulated, whichever came first. Low-activity samples were counted for up to 75 min or until 6400 disintegrations (2.5% 2σ) were accumulated.

Effect of P-gp blockade on DPC 333 pharmacokinetics. Male Sprague-Dawley rats (approximately 250 g at study initiation), fitted with indwelling jugular cannulas for the collection of blood, were obtained from Charles River Laboratories Inc. Before conduct of dosing studies, animals were anesthetized
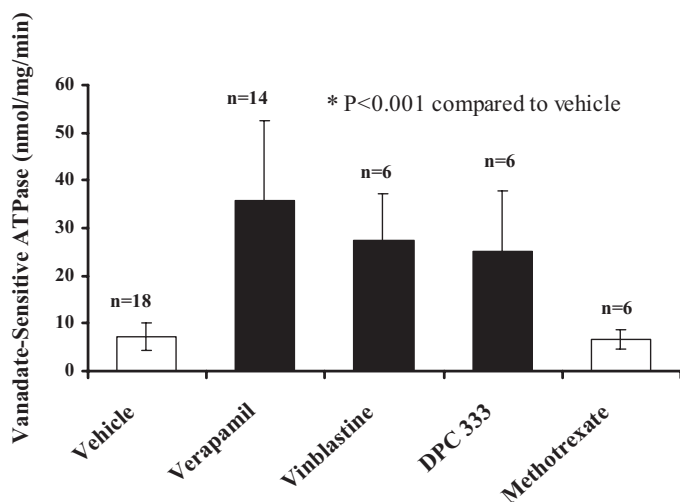
FIG. 2. Stimulation of human P-glycoprotein-ATPase activity by DPC 333, verapamil, and other molecules (20 mM).

with pentobarbital, and duodenal catheters were implanted for intestinal delivery of solutions. Approximately 10 min before administration of test compound, one group of three rats was pretreated with verapamil (1 mg/kg), a known P-gp inhibitor (Chang et al., 2006), and another group of three rats was administered saline. Following pretreatment each rat then received a single p.o. gavage dose of DPC 333 of 15 mg/kg. Blood was collected from each animal at 0.083, 0.17, 0.25, 0.5, 1.5, and 2 h following administration of test material.

Plasma was prepared, and the concentration of DPC 333 was determined via liquid chromatography/tandem mass spectrometry. Plasma concentration versus time data were then analyzed by noncompartmental methods using Win-Nonlin (Mountain View, CA).

In Situ Intestinal Perfusion. Sprague-Dawley rats previously fitted with portal vein and bile duct cannulas were supplied by Charles River Canada Inc. Ketamine and xylazine were purchased from Fort Dodge Lab Inc. (Fort Dodge, IA). Krebs-Ringer bicarbonate buffer components (KH_2PO_4, $MgSO_4$, NaCl, KCl, $CaCl_2 \cdot 2H_2O$, $NaHCO_3$, glucose) were purchased from Sigma Chemical Co. (St. Louis, MO).

A single-pass intestinal perfusion technique was used. Surgery was adapted from that described by Wang et al. (1997, 1999). Briefly, male Sprague-Dawley rats (~200 g) prefitted with indwelling jugular vein cannulas before surgery were anesthetized with ketamine/xylazine (100:7 mg/kg). The fur from the abdominal region was removed with clippers; the skin was cleaned with alcohol; and the rat was then placed in a supine position on a heating pad within a chamber designed to maintain body temperature throughout the experiment. The apparatus, which was constructed in-house, consisted of a Lucite (Lucite International, Southampton, UK) housing with thermostatically controlled electric heaters to maintain the rat and all the perfusion solutions at 37°C. Once the rat was positioned, laparotomy was performed, and the small intestine was fitted at inlet and outlet with polished glass tubing to allow for perfusion of the interior with Krebs-Ringer buffer (pH 7.4, 37°C). The intestinal lumen was then gently flushed to remove intestinal contents. The proximal end of the intestine was connected to a perfusion syringe on a variable speed compact infusion pump, and the interior of the intestine was perfused with Krebs-Ringer buffer at a flow rate of 250 μl/min. Effluent was collected from the glass tubing at the distal end of the intestine. The intestine was carefully arranged and continuously monitored to avoid kinks and ensure a consistent flow. Saline-soaked cotton gauze was used to cover opened body cavities to prevent loss of fluids. Once the intestinal effluent flow had been established, [^{14}C]DPC 333 (15 mg/kg, 14.4 μCi) was then administered i.v. via the indwelling jugular vein cannula. Following administration of test substance, intestinal effluent samples were collected into preweighed glass vials every 15 min for up to 180 min. Blood samples were sampled at times of effluent collection time points for plasma analysis of parent compound. Blood volume was maintained by immediately transfusing back into the cannula an equal volume of blood taken from donor rats. At the end of the experiment, the remaining intestinal perfusate solution was expelled by infusing air and then flushing with normal saline through the intestinal segment. Aliquots of the collected material were analyzed for total radiochemical content by liquid scintillation spectrometry before characterization of radiochemical profile by HPLC.

Analysis of intestinal perfusate and plasma. DPC 333 was determined in plasma and intestinal perfusate by HPLC radiochemical analysis. Before HPLC analysis, perfusate or plasma samples were mixed with an equal volume of acetonitrile (EM Science, Gibbstown, NJ) and vortexed for approximately 30 s. The mixtures were centrifuged at approximately 3000g for 10 min, and the supernatants were filtered with a 0.45 μM syringe filter (Whatman Inc., Florham Park, NJ). Aliquots (100 μl) were then analyzed for parent compound by HPLC/flow-through radiochemical detection. Briefly, the chromatographic system consisted of a Hewlett Packard (Palo Alto, CA) model 1100 chromatography system (pumps, controllers, and injectors), a Metachem Polaris (Ventura, CA) C_{18}-A 2 × 150-mm column, and a linear gradient mobile phase at a flow rate of 0.4 ml/min. Mobile phase A was 10 mM ammonium formate, pH 7.4 (Fisher Scientific Co., Pittsburgh, PA), and mobile phase B was acetonitrile. The gradient conditions started at 6% mobile phase B, ramping linearly to 11% B over 10 min, then to 45% B over 6 min, then to 61% B over 2 min, then held at 61% B over 2 min, and finally ramping to 71% B over the final 2 min. Column eluent was monitored via IN/US Systems (Tampa, FL) β-RAM flow-through radioactivity detector outfitted with a 1-ml liquid/liquid flow-through cell. Column eluent was mixed with Flow-Scint (Packard Instruments) at a 1:4 ratio before detection.

Results

In Vitro Experiments. The role of DPC 333 as a P-gp substrate was suggested in verapamil-activated vanadate-sensitive human P-gp
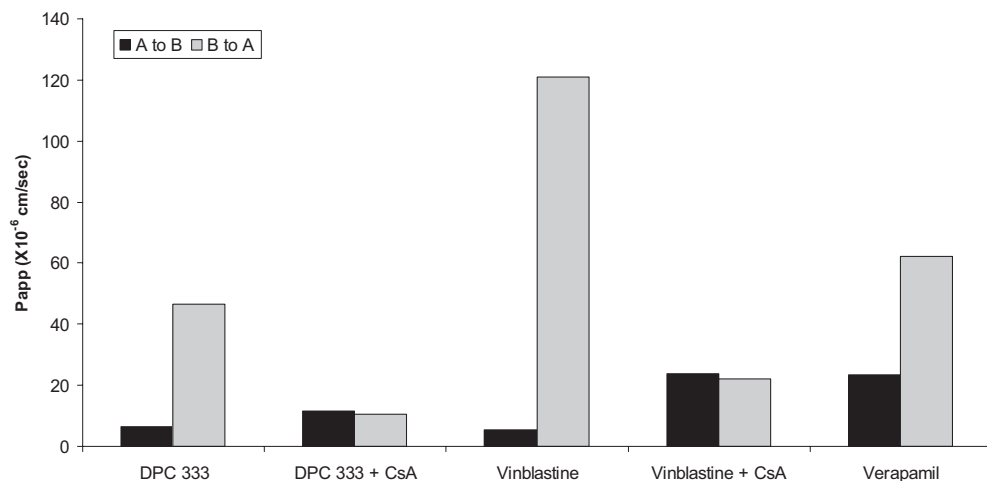

FIG. 3. Permeability of DPC 333 and other molecules in monolayers of MDCK II cells transfected with MDR1.
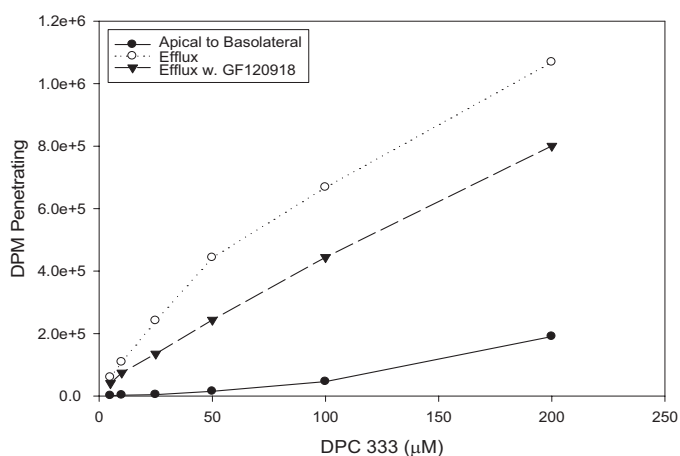
FIG. 4. Distribution of [14C]DPC 333-derived radioactivity in Caco-2 monolayers.

ATPase activity assays (Fig. 2). DPC 333 activity in this assay was similar to that of verapamil and vinblastine, two known P-gp substrates. In MDCK cells stably transfected with MDR1 and DPC 333, the transport from B→A reservoirs exceeded the transport from A→B by approximately 7-fold (Fig. 3). This ratio was reduced to 1 by addition of the P-gp inhibitor cyclosporin A.

To investigate the potential for intestinal efflux or elimination of DPC 333, [14C]DPC 333 was incubated against confluent Caco-2 monolayers. Initial concentrations of [14C]DPC 333 in either apical (A) or basolateral (B) donor reservoirs was 0 to 200 μM (0.5 μCi/incubation). After 2-h incubation, radiochemical content in receptor reservoirs was determined. In Caco-2 monolayers, DPC 333 was transported from A to B or B to A reservoirs in a concentration-dependent manner (Fig. 4). DPC 333 transport from B→A reservoirs was concentration-dependent and saturable, suggesting an active transport mechanism (Fig. 4). Transport from the basolateral to apical reservoir was partially blocked with GF120918, suggesting that P-gp or BCRP played a role in B→A efflux of DPC 333.

When DPC 333 was incubated with isolated rat ileum in Ussing chambers, B→A efflux greatly exceeded A→B (Fig. 5A). Furthermore, B→A efflux was nearly completely blocked by GF120918 (Fig. 5B). These in vitro data taken together suggest that DPC 333 is a P-gp and/or BCRP substrate and that these transporters may contribute to the basolateral to apical flux in the intestine.

Rat and Mouse Whole-Body Autoradiography. An autoradiograph (mouse at 2 min postdose) and mouse tissue concentration data
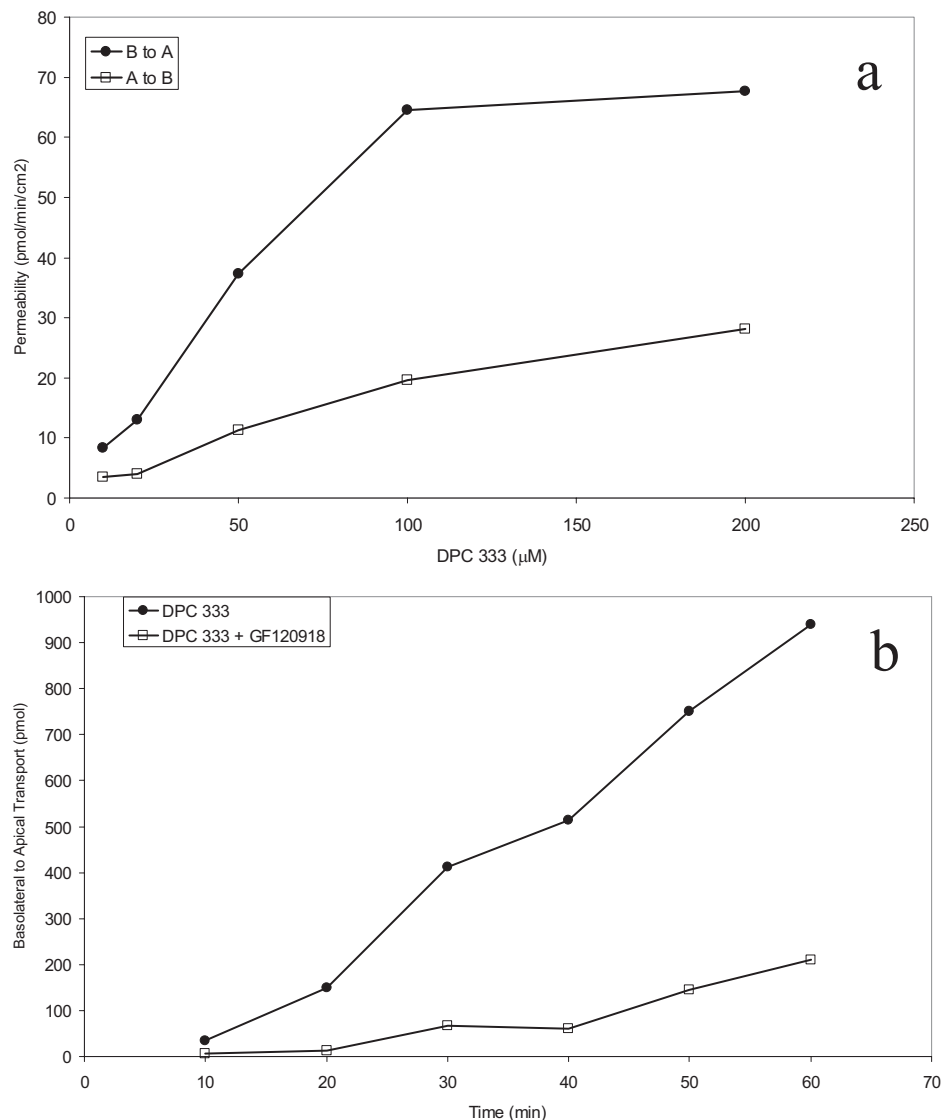

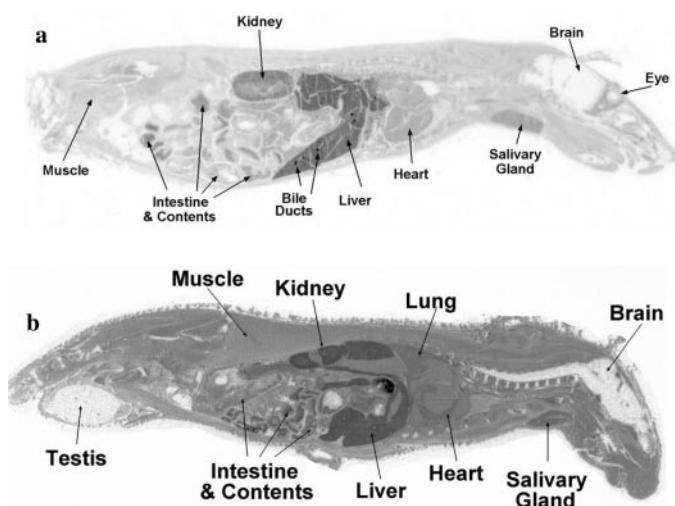FIG. 5. Permeability of DCP 333 in rat ileal mucosal sections.

FIG. 6. Whole-body autoradiographs of an intact mouse (A) and a bile duct–cannulated rat (B) sacrificed at 2 min after an i.v. dose of [^{14}C]DPC 333.

are presented in Fig. 6A and Table 1, respectively. Concentrations of [^{14}C]DPC 333-derived radioactivity were generally well distributed to all the tissues in mice at early time points (2 min to 1 h) except brain and spinal nerve cord, which showed little or no radioactivity. Highest concentrations were present in liver, gall bladder contents, kidney, heart, salivary gland, lacrimal gland, lung, gastrointestinal (GI) tract, and intestinal contents. After 2 h, high concentrations of radioactivity were observed in the liver and contents of the gall bladder and GI tract only. By 24 h postdose, low levels of radioactivity were present in the liver, heart, kidney, blood, and lung, and remaining tissue showed none or only trace levels. These QWBA data suggest that [^{14}C]DPC 333 is well distributed throughout the bodies of normal mice. However, penetration into brain, spinal cord, and bone was not shown in this experiment. The study showed that [^{14}C]DPC 333 is cleared via renal and biliary excretion and possibly intestinal secretion as a result of radioactivity observed in the GI tract.

Figure 6B is a whole-body autoradiograph of a bile duct-cannulated rat 2 min after i.v. dosing. Rat tissue concentrations are presented in Table 2. In general, concentrations of [^{14}C]DPC 333-derived radioactivity were well distributed to all the tissues in rats at all the time points (2 min to 1 h) except brain and spinal nerve cord, which showed little or no radioactivity. Highest concentrations were present in liver, kidney, heart, pituitary gland, salivary gland, lacrimal gland, lung, GI tract, and intestinal contents. These QWBA results suggest that [^{14}C]DPC 333 is well distributed throughout the body of rats in a manner similar to the mouse. The radioactivity observed in the contents of the GI tract was strong evidence to support the hypothesis of intestinal excretion as all the bile was diverted away from the bile duct and thus from entering the intestine.

Effect of P-gp/BCRP Blockade on DPC 333 Mass Balance and Pharmacokinetics in Vivo. To further investigate this hypothesis, [^{14}C]DPC 333 was administered i.v. to bile duct–cannulated rats, and the excretion of radioactivity was determined in bile, urine, and feces. Bile cannulation removes the contribution of biliary excretion of radioactivity to gut contents. Of the four animals treated with test compound, two rats were pretreated with 25 mg/kg GF120918 24 and 1 h before administration of [^{14}C]DPC 333 to determine the effect of P-gp/BCRP blockade on ^{14}C excretion. The majority of radioactivity administered i.v. to control rats was distributed between urine (40%) and bile (56%) 48 h postdose (Table 3). However, approximately 5% of an i.v. dose was recovered in the feces within 48 h, suggesting that

the intestine served as an organ of excretion for DPC 333 and/or its equivalents. In the GF120918-pretreated animals, fecal radioactivity was reduced to approximately 2% of total dose. Biliary equivalents (~54%) were reduced relative to untreated animals. Urinary equivalents (~45%) were increased by an amount roughly concomitant to the combined reduction in fecal and biliary routes of elimination.

To investigate the role of P-gp as the principal efflux transporter of DPC 333, rats were pretreated with verapamil, which inhibits P-gp. Pretreatment of rats with verapamil resulted in a nearly 6-fold increase in DPC 333 C_{max} (Table 4). Overall exposure (area under the plasma concentration-time curve) increased 1.6-fold following verapamil pretreatment relative to saline controls. Together, these data suggest that intestine plays a role in the elimination of DPC 333 in rats and that P-gp may contribute predominantly to this phenomenon.

In Situ Perfused Rat Intestine Studies. To estimate the contribution of the intestine to the total clearance of DPC 333, [^{14}C]DPC 333 was administered i.v. to rats in the in situ perfused small intestine model. Within 3 h post-i.v. dose, 17% of the total radioactivity administered was collected in the intestinal effluent. Approximately 53 and 6% of the dose was recovered in the bile and urine, respectively. Total recovery was 76.6% of total dose by 3 h. Distribution and recovery were similar to that measured in the intact animals by 3 h in separate distribution studies conducted in bile duct–cannulated rats. At early time points intestinal effluent radioactivity was predominantly parent molecule (data not shown). By 2 h postadministration, a single unidentified metabolite began to contribute to the profile, but through 4 h postdose parent compound in the effluent comprised 50 to 75% of total radioactivity (data not shown). Parent compound was not detected in urine. Plasma radioactivity was predominantly parent compound at 15 min postdose, but the contribution of parent decreased to less than 20% by 3 h postadministration. Profiles of plasma and intestinal effluent were qualitatively similar, with parent molecule and a single, unidentified metabolite the only detectable peaks. Systemic clearance of 2.1 l/h/kg, estimated from these plasma data (Table 4), closely matched that measured in similar studies in intact animals (2.7 l/h/kg) (Qian et al., 2007). Intestinal clearance was estimated at 0.2 l/h/kg, approximately 10% of measured total systemic clearance.

Discussion

The results of these studies suggest that the intestine is an organ of DPC 333 excretion in rodents. Additionally, our data suggest that the ATP-binding cassette protein P-gp or BCRP mediates this excretion in part or wholly. In mouse and rat QWBA distribution studies, significant portions of [^{14}C]DPC 333-derived radioactivity administered i.v. were detected along the gut lumen within 2 to 5 min postdose, directly suggesting a role of the intestine in elimination of DPC 333 or its equivalents in vivo. By approximately 1 h, 15 and 17% of the administered radioactivity was detected in the intestinal contents of rats and mice, respectively.

In mice, by 2 min postadministration, radioactivity was distributed throughout the small intestine, and after 2 h, high concentrations of radioactivity were observed in the liver, gall bladder, and GI tract only. Because of the fasted state of the mice and the rapid appearance of radioactivity throughout the entire length of the intestine, the contribution of biliary excretion to the intestinal radioactivity measured initially was probably minimal. However, the presence of intact bile ducts in these animals suggests that the contribution of biliary excretion to intestinal radioactivity could not be entirely ruled out. Repetition of these results in the bile duct–cannulated rat QWBA studies was strong evidence to support the hypothesis of intestinal excretion because all the bile was diverted away from the bile duct and thus prevented from entering the intestine.

TABLE 1

Concentration of radioactivity in blood and tissues at specified times postdose determined by whole-body autoradiography for female mice following i.v. administration of [^{14}C]DPC 333

Results are in nanocuries per gram tissue.

Tissue[a]	Animal Sacrifice Time									
	2 min	5 min	15 min	30 min	1 h	2 h	4 h	6 h	12 h	24 h
Blood	864.6	654.2	204.6	118.6	37.30	28.10	19.70	23.20	14.60	11.40
Bone marrow	529.4	457.5	161.6	63.40	20.20	14.90	8.300	10.40	6.000	3.200
Brain	14.40	10.80	4.000	2.300	0.9000	0.7000	0.5000	0.6000	0.4000	0.3000
Brown fat	497.1	485.6	170.3	90.70	36.80	20.00	12.00	14.80	5.700	3.600
Gall bladder contents	N.R.	25,420	15,340	37,810	32,590	44,500	17,350	N.R.	N.R.	N.R.
Heart	1061	559.3	121.0	54.10	15.10	12.90	7.700	11.00	5.500	3.800
Kidney	1732	1915	692.0	324.3	56.80	42.30	31.80	37.80	14.00	7.400
Lacrimal gland	1023	620.0	187.4	N.R.	27.30	16.80	N.R.	10.20	4.800	2.200
Liver	3135	2793	1049	597.6	170.1	106.6	98.20	95.20	36.50	17.60
Lymph nodes	144.4	298.8	175.2	112.8	67.90	46.00	13.40	8.000	10.50	4.800
Lung	853.7	347.7	196.4	92.70	26.30	22.70	17.60	19.20	16.70	7.500
Salivary gland	1287	805.8	260.0	106.9	24.90	21.50	16.50	15.90	6.500	3.300
Skeletal muscle	229.3	171.3	80.70	28.20	5.500	2.90	2.100	2.400	1.500	0.9000
Skin	136.0	169.4	92.80	59.00	19.30	11.30	5.400	8.100	4.800	3.900
Spleen	343.0	433.3	266.4	128.4	N.R.	42.60	21.60	17.90	7.600	4.400
White fat	147.0	103.5	69.40	43.10	19.70	11.20	6.200	3.400	1.900	1.800

N.R., not represented (tissue or organ not present in original section).
LLOQ = 1.263 nCi/g.
[a] Intestinal contents exceeded upper linear range and therefore were not quantitated.

TABLE 2

Concentration of radioactivity in blood and tissues at specified times postdose determined by whole-body autoradiography for bile duct–cannulated male rats following i.v. administration of [^{14}C]DPC 333

Results are in nanocuries per gram tissue.

Tissue	Animal Sacrifice Time		
	2 min	5 min	1 h
Adrenal gland	1449	1152	325.6
Blood	419.3	346.1	129.6
Bone marrow	461.1	320.1	262.3
Brown fat	N.S.	614.0	188.5
Brain	13.96	10.43	4.689
Brain ventricle	327.7	269.2	N.S.
Epididymis	46.80	55.82	78.88
Harderian gland	232.6	205.2	383.9
Heart	677.2	462.9	160.7
Intestine	1110	879.9	2590
Kidney	1534	1010	1031
Liver	1253	1759	465.6
Lung	418.2	486.7	230.7
Lymph node	N.S.	169.5	N.S.
Muscle	454.7	199.4	187.6
Pancreas	639.5	504.7	282.6
Pituitary gland	796.3	432.5	292.3
Prostate	133.2	197.0	160.5
Salivary	626.9	401.2	260.8
Seminal vesicle	23.88	14.97	29.77
Skin	156.8	164.4	249.1
Spleen	389.4	634.9	536.4
Stomach (glandular)	690.6	725.3	2309
Stomach (nonglandular)	123.7	141.1	170.3
Testis	9.302	13.69	31.23
Thymus	195.6	115.7	159.7
Thyroid	640.7	338.2	209.6
White fat	176.45	137.2	203.9
LLOQ (small tissues)	4.197	2.951	3.349
LLOQ (large tissues)	3.437	2.548	2.344

N.S., not sampled (sample shape not discernable from background).

TABLE 3

Distribution of radioactivity 48 h following i.v. administration of [^{14}C]DPC 333 (15 mg/kg) to naïve or GF120918-pretreated rats

	Naïve			Pretreated		
	Rat 1	Rat 2	Average	Rat 1	Rat 2	Average
Feces	5.9	4.4	5.1	2.5	1.1	1.8
Urine	47.8	32.2	40.0	47.8	42.7	45.3
Bile	48.0	63.9	56.0	49.3	58.3	53.8
Sum	101.7	100.4	101.1	99.6	102.0	100.8

TABLE 4

Pharmacokinetic parameters of DPC 333 following p.o. administration of DPC 333 (15 mg/kg) to rats following intraduodenal infusion with verapamil (1 mg/kg) or saline

Treatment	C_{max}	-Fold Increase in C_{max}	AUC_{0-120}	-Fold Increase in AUC_{0-120}
	nM		*nM · min*	
Saline	106		5388	
Verapamil	605	5.7	8704	1.6

perfused intestine studies. This suggests that there may be reabsorption processes operative, perhaps in the cecum or colon. That the potent P-gp/BCRP inhibitor GF120918 was capable of partially blocking the appearance of fecal radioactivity suggested that the intestinal excretion of equivalents in vivo was mediated at least in part by ATP-binding cassette transporters P-gp or BCRP. At the intestinal level, the efflux of DPC 333 was shown to be modulated significantly by verapamil, which inhibits P-gp (Chang et al., 2006) but does not inhibit BCRP (Zhang et al., 2005). Verapamil pretreatment increased DPC 333 C_{max} almost 6-fold and area under the plasma concentration-time curve by 60% in rats. Although BCRP involvement cannot be ruled out completely, these data suggest strongly that P-gp plays a role in DPC 333 efflux.

Results of in vitro studies conducted with human MDR1, Caco-2 monolayers, and isolated rat intestinal mucosa agree with in vivo data suggesting that DPC 333 was a P-gp substrate. DPC 333 was subject to basolateral to apical efflux in both Caco-2 monolayers, MDR1-transfected MDCK monolayers, and rat ileal mucosa, and this efflux

In separate studies, [^{14}C]DPC 333-derived radioactivity was detected in the feces of bile duct–cannulated rats following i.v. administration of [^{14}C]DPC 333, supporting the WBA results. In this study, 5% of the dose was recovered in the feces at 48 h compared with 15 to 17% measured in small intestine by 1 h in WBA and in situ

TABLE 5

Pharmacokinetic parameters derived following i.v. administration of [^{14}C]DPC 333 (15 mg/kg) to rats in the in situ perfused intestine model

Parameter	Rat 1	Rat 2	Rat 3	Mean	S.D.
AUC, nM · h	10,029	26,060	15,442	17,177	8155
nmol Dosed	6565	5878	5290	5911	638
nmol Excreted	652	895	680	742	133
Rat weight, kg	0.20	0.21	0.19	0.20	0.01
Cl_{sys}, l/h/kg	3.3	1.1	1.9	2.07	1.11
Cl_{si}, l/h/kg	0.3	0.2	0.2	0.24	0.08

was nearly completely blocked with GF120918 and cyclosporin. Kinetic analysis of the Caco-2 and ileal section data gave K_ms of 25 and 46 μM, respectively. These data suggested that the intestine may have a relatively high capacity for basolateral to apical clearance of DPC 333.

The contribution of the intestine to the total clearance of DPC 333 was estimated from data generated in the rat in situ perfused small intestine model. Approximately 17% of total radioactivity administered was excreted into the intestinal lumen within 3 h post-i.v. administration and 12% of the dose as parent. Intestinal clearance of approximately 0.21 l/h/kg suggested that the intestine contributed to approximately 10% of total systemic clearance (Table 5). However, a careful kinetic analysis of the data generated in this model suggests

that DPC 333 clearance may exceed that measured in the in situ perfused intestine model. That is, the data support the possibility that nearly all the DPC 333-derived radioactivity measured was initially excreted as parent by P-gp or BCRP.

A plot of plasma DPC 333 concentration versus rate of luminal excretion of DPC 333 and equivalents yielded a hyperbolic curve, suggesting a saturable excretion mechanism (Fig. 7A). This would be expected, given the strong data supporting the transporter-mediated flux of DPC 333. This suggests that the rate of all the equivalents appearing in the lumen is dependent solely on plasma parent concentration. If metabolite were actively excreted into the lumen, then the rate of its appearance in the lumen would also be a function of plasma metabolite concentration, saturable, and therefore hyperbolic across a large concentration range. However, luminal appearance of "metabolite" was independent of plasma concentration (Fig. 7B).

The intestinal elimination rate data and plasma concentration data were fit to a combined pharmacokinetic/hyperbolic elimination model. This model accurately predicted intestinal excretion of parent and total equivalents (Fig. 8).

The above analysis suggests that DPC 333 equivalents in the lumen were initially excreted as parent via a transporter and then subsequently metabolized in the lumen, presumably by brush-border enzymes. This phenomenon is seen with *p*-aminobenzoic acid, *p*-aminosalicylic acid, and sulfanilic acid (Yasuhara et al., 1984), which are acetylated by intestinal acetyltransferases following luminal secretion. Pang et al. (1986) have also shown that acetaminophen is excreted into the intestine and then glucuronidated luminally. The data cannot rule out the possibility that excreted DPC 333 is reabsorbed into mucosal cells, metabolized, and then the metabolite re-excreted. This phenomenon has been shown with *p*-nitrophenol in the rat (Fischer et al., 1995; Rafiei et al., 1996).

To summarize, the above data taken in whole would suggest that in rodents DPC 333 is cleared via the intestine in part or in whole via the transporter P-gp or BCRP. In rats, DPC 333 intestinal clearance is estimated to be a minimum of 12% of systemic clearance (0.35 l/h/kg, based on luminal parent only) with a maximum of approximately 18%
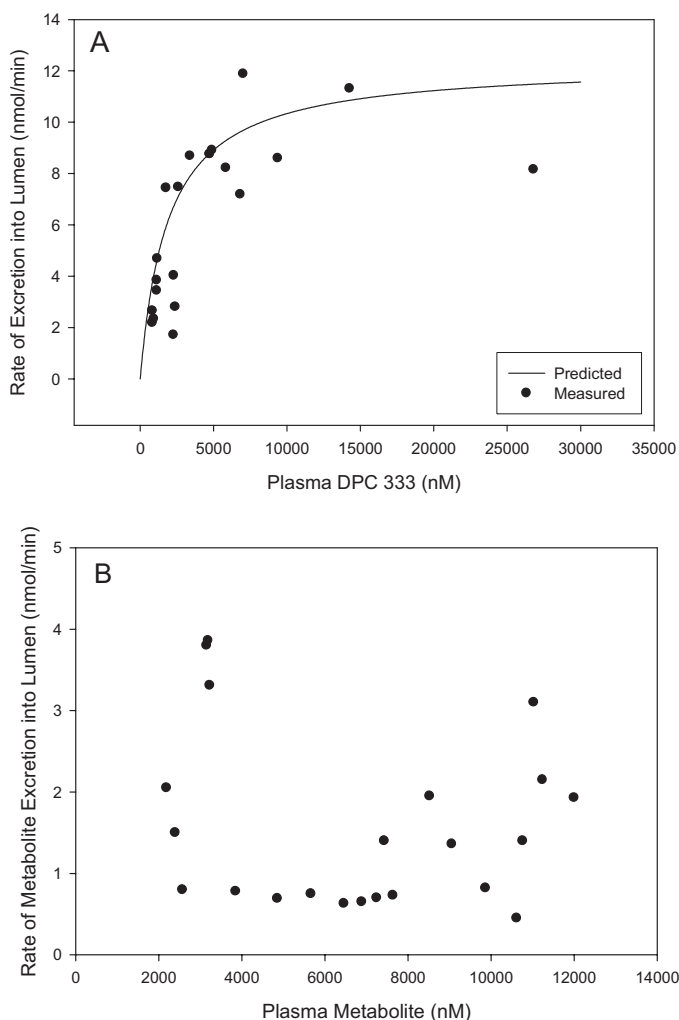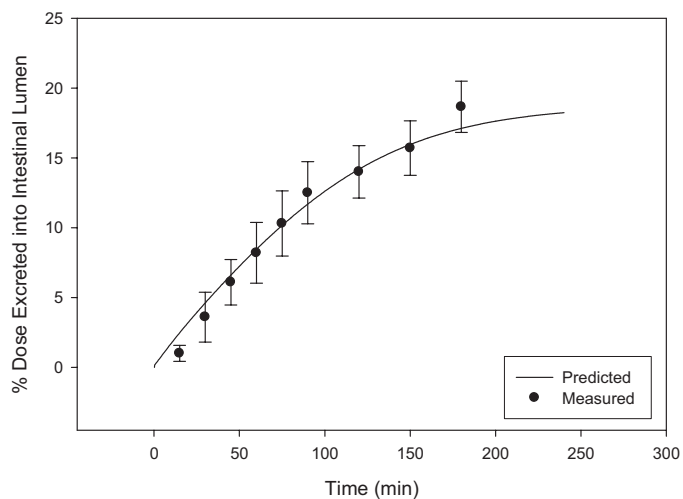

FIG. 7. Effect of plasma concentration of DPC 333 (A) or metabolite (B) on the elimination of DPC 333 equivalents into intestinal lumen following i.v. administration of DPC 333 in the in situ perfused rat intestine model.

FIG. 8. Predicted versus measured luminal DPC 333 and equivalents following i.v. administration of [^{14}C]DPC 333 (15 mg/kg) in the in situ perfused rat intestine model. Luminal excretion predicted by the following expression:

$$\text{nmoles} = \left(\frac{V_{max} \times C_{plasma}}{EC_{50} + C_{plasma}} \right) \times \Delta t \text{ where } C_{plasma} = \left(\frac{\text{dose}}{15} \right) (Ae^{-\alpha t} + Be^{-\beta t})$$

and V_{max} = 11.8 nmol/min, EC_{50} = 2266 nM, A = 163,399, α = 0.21 h^{-1}, B = 18,824, β = 0.020 h^{-1}, and dose = 15 mg/kg.

(0.52 l/h/kg, based on total equivalents) of systemic clearance. If indeed this elimination pathway exists in humans and the relative contribution of the intestine to total clearance is roughly similar to that of rodents, then this suggests a potential impact on total clearance as a result of intestinal interactions with other P-gp or BCRP substrates.

References

Allen JD, Brinkhuis RF, Wijnholds J, Schinkel AH (1999) The mouse Bcrp1/Mxr/Abcp gene: amplification and overexpression in cell lines selected for resistance to topotecan, mitoxantrone, or doxorubicin. *Cancer Res* **59:**4237–4241.

Artursson P, Ungell AL, and Lofroth JE (1993) Selective paracellular permeability in two models of intestinal absorption: cultured monolayers of human intestinal epithelial cells and rat intestinal segments. *Pharm Res* **10:**1123–1129.

Breedveld P, Pluim D, Cipriani G, Wielinga P, van Tellingen O, Schinkel AH, Schellens JH (2005) The effect of Bcrp1 (Abcg2) on the in vivo pharmacokinetics and brain penetration of imatinib mesylate (Gleevec): implications for the use of breast cancer resistance protein and P-glycoprotein inhibitors to enable the brain penetration of imatinib in patients. *Cancer Res* **65:**2577–2582.

Caldwell JH, Caldwell PB, Murphy JW, and Beachler CW (1980) Intestinal secretion of digoxin in the rat. Augmentation by feeding activated charcoal. *Naunyn Schmiedebergs Arch Pharmacol* **312:**271–275.

Chang JH, Kochansky CJ, and Shou M (2006) The role of P-glycoprotein in the bioactivation of raloxifene. *Drug Metab Dispos* **34:**2073–2078.

Chay S and Poland R (1994) Comparison of quantitative whole-body autoradiography and tissue dissection techniques in the evaluation of the tissue distribution of [14C]Daptomycin in rats. *J Pharm Sci* **83:**1294–1299.

Dautrey S, Felice K, Petiet A, Lacour B, Carbon C, and Farinotti R (1999) Active intestinal elimination of ciprofloxacin in rats: modulation by different substrates. *Br J Pharmacol* **127:**1728–1734.

de Bruin M, Miyake K, Litman T, Robey R, Bates SE (1999) Reversal of resistance by GF120918 in cell lines expressing the ABC half-transporter, MXR. *Cancer Lett* **146:**117–126.

Drüeke T, Hennessen U, Nabarra B, Ben Nasr L, Lucas PA, Dang P, Thomasset M, Lacour B, Coudrier E, and McCarron DA (1990) Ultrastructural and functional abnormalities of intestinal and renal epithelium in the SHR. *Kidney Int* **37:**1438–1448.

Eisenblätter T, Hüwel S, Galla HJ (2003) Characterisation of the brain multidrug resistance protein (BMDP/ABCG2/BCRP) expressed at the blood-brain barrier. *Brain Res* **971:**221–31.

Fischer E, Rafiel A, and Bojcsev S (1995) Intestinal elimination of p-nitrophenol in the rat. *Acta Physiol Hung* **83:**355–362.

Greiner B, Eichelbaum M, Fritz P, Kreichgauer H, Von Richter O, Zundler J, and Kroemer HK (1999) The role of intestinal p-glycoprotein in the interaction of digoxin and rifampin. *J Clin Invest* **104:**147–153.

Hall SD, Thummel KE, Watkins PB, Lown KS, Benet LZ, Paine MF, Mayo RR, Turgeon DK, Bailey DG, Fontana RJ, et al. (1999) Molecular and physical mechanisms of first-pass extraction. *Drug Metab Dispos* **27:**161–166.

Hassan NJ, Pountney DJ, Ellis C, Mossakowska DE (2006) BacMam recombinant baculovirus in transporter expression: a study of BCRP and OATP1B1. *Protein Expr Purif* **47:**591–598.

Hyafil F, Vergely C, Du Vignaud P, Grand-Perret T (1993) In vitro and in vivo reversal of multidrug resistance by GF120918, an acridonecarboxamide derivative. *Cancer Res* **53:**4595–4602.

Hyde SC, Emsley P, Hartshorn MJ, Mimmack MM, Gileadi U, Pearce SR, Gallagher MP, Gill DR, Hubbard RE, and Higgins CF (1990) Structural model of ATP-binding proteins associated with cystic fibrosis, multidrug resistance and bacterial transport. *Nature* **346:**362–365.

Imbert F, Jardin M, Fernandez C, Gantier JC, Dromer F, Baron G, Mentre F, Van Beijsterveldt L, Singlas E, Gimenez F (2003) Effect of efflux inhibition on brain uptake of itraconazole in mice infected with Cryptococcus neoformans. *Drug Metab Dispos* **31:**319–325.

Lagas JS, Vlaming ML, van Tellingen O, Wagenaar E, Jansen RS, Rosing H, Beijnen JH, and Schinkel AH (2006) Multidrug resistance protein 2 is an important determinant of paclitaxel pharmacokinetics. *Clin Cancer Res* **15:**6125–6132.

Leusch A, Volz P, Muller G, Wagner A, Sauer A, Greischel A, and Roth W (2002) Altered drug disposition of the platelet activating factor antagonist apafant in mdr1a knockout mice. *Eur J Pharm Sci* **16:**119–128.

Li J, Zhou S, Huynh H, and Chan E (2005) Significant intestinal excretion, one source of variability in pharmacokinetics of COL-3, a chemically modified tetracycline. *Pharm Res* **22:**397–404.

Mayer U, Wagenaar E, Beijnen JH, Smit JW, Meijer DKF, Van Asperen J, Borst P, and Schinkel AH (1996) Substantial excretion of digoxin via the intestinal mucosa and prevention of long-term digoxin accumulation in the brain by the mdr1a p-glycoprotein . *Br J Pharmacol* **119:**1038–1044.

Merino G, Jonker JW, Wagenaar E, Pulido MM, Molina AJ, Alvarez AI, Schinkel AH (2005)

Transport of anthelmintic benzimidazole drugs by breast cancer resistance protein (BCRP/ABCG2). *Drug Metab Dispos* **33:**614–618.

Pang KS, Yuen V, Fayz S, te Koppele JM, and Mulder GJ (1986) Absorption and metabolism of acetaminophen by the in situ perfused rat small intestine preparation. *Drug Metab Dispos* **14:**102–111.

Perdaems N, Caunes N, Canal P, and Chatelut E (1999) Possible excretion of etoposide via the intestinal mucosa. *Cancer Chemother Pharmacol* **43:**520–521.

Qian M, Bai S, Brogdon B, Wu JT, Liu W, Covington M, Vaddi K, Newton RC, Deng Y, Garner CE, et al (2007) Pharmacokinetics and pharmacodynamics of DPC 333, a potent and selective inhibitor of tumor necrosis factor-α converting enzyme in rodents, dogs, chimpanzees and humans. *Drug Metab Dispos* **35:**1916–1925.

Rabbaa L, Dautrey S, Colas-Linhart N, Carbon C, and Farinotti R (1996) Intestinal elimination of ofloxacin enantiomers in the rat: evidence of a carrier-mediated process. *Antimicrob Agents Chemother* **40:**2126–2130.

Rafiei A, Bojcsev S, and Fischer E (1996) Dose-dependent intestinal and hepatic glucuronidation and sulfatation of p-nitrophenol in the rat. *Acta Physiol Hung* **84:**333–335.

Rautio J, Humphreys JE, Webster LO, Balakrishnan A, Keogh JP, Kunta JR, Serabjit-Singh CJ, Polli JW (2006) In vitro p-glycoprotein inhibition assays for assessment of clinical drug interaction potential of new drug candidates: a recommendation for probe substrates. *Drug Metab Dispos* **34:**786–792.

Salphati L and Benet LZ (1998) Effects of ketoconazole on digoxin absorption and disposition in rat. *Pharmacology* **56:**308–313.

Sarkadi B, Price EM, Boucher RC, Germann UA, and Scarborough GA (1992) Expression of the human multidrug resistance cDNA in insect cells generates a high activity drug-stimulated membrane ATPase. *J Biol Chem* **267:**4854–4858.

Smit JW, Schinkel AH, Muller M, Weert B, and Meijer DK (1998a) Contribution of the murine mdr1a p-glycoprotein to hepatobiliary and intestinal elimination of cationic drugs as measured in mice with an mdr1a gene disruption. *Hepatology* **27:**1056–1063.

Smit JW, Schinkel AH, Weert B, and Meijer DK (1998b) Hepatobiliary and intestinal clearance of amphiphilic cationic drugs in mice in which both mdr1a and mdr1b genes have been disrupted. *Br J Pharmacol* **124:**416–424.

Sparreboom A, van Asperen J, Mayer U, Schinkel AH, Smit JW, Meijer DK, Borst P, Nooijen WJ, Beijnen JH, and van Tellingen O (1997) Limited oral bioavailability and active epithelial excretion of paclitaxel (taxol) caused by p-glycoprotein in the intestine. *Proc Natl Acad Sci U S A* **94:**2031–2035.

Ullberg S (1954) Studies on the distribution and fate of 35S-labeled benzylpenicillin in the body. *Acta Radiol Suppl* **118:**1–110.

Ungell AL, Nylander S, Bergstrand S, Sjoberg A, and Lennernas H (1998) Membrane transport of drugs in different regions of the intestinal tract of the rat. *J Pharm Sci* **87:**360–366.

van Asperen J, van Tellingen O, and Beijnen J (2000) The role of mdr1a P-glycoprotein in the biliary and intestinal secretion of doxorubicin and vinblastine in mice. *Drug Metab Dispos* **28:**264–267.

Villanueva SS, Ruiz ML, Soroka CJ, Cai SY, Luquita MG, Torres AM, Sanchez Pozzi EJ, Pellegrino JM, Boyer JL, Catania VA, et al. (2006) Hepatic and extrahepatic synthesis and disposition of dinitrophenyl-S-glutathione in bile duct-ligated rats. *Drug Metab Dispos* **34:**1301–1309.

Wang Y, Aun R, and Tse FL (1997) Absorption of D-glucose in the rat studied using in situ intestinal perfusion: a permeability index approach. *Pharm Res* **14:**1563–1567.

Wang Y, Lin H, Tullman R, Jewell CF Jr, Weetall ML, and Tse FL (1999) Absorption and disposition of a tripeptoid and a tetrapeptide in the rat. *Biopharm Drug Dispos* **20:**69–75.

Westphal K, Weinbrenner A, Zschiesche M, Franke G, Knoke M, Oertel R, Fritz P, von Richter O, Warzok R, Hachenberg T, et al. (2000) Induction of P-glycoprotein by rifampin increases intestinal secretion of talinolol in human beings: a new type of drug/drug interaction. *Clin Pharmacol Ther* **68:**345–355.

Yasuhara M, Kurosaki Y, Kimura T, and Sezaki H (1984) Drug elimination function of rat small intestine: metabolism and intraluminal excretion. *Biochem Pharmacol* **33:**3131–3136.

Yeboah D, Sun M, Kingdom J, Baczyk D, Lye SJ, Matthews SG, Gibb W (2006) Expression of breast cancer resistance protein (BCRP/ABCG2) in human placenta throughout gestation and at term before and after labor. *Can J Physiol Pharmacol* **84:**1251–1258.

Zalups RK (1998) Intestinal handling of mercury in the rat: implications of intestinal secretion of inorganic mercury following biliary ligation or cannulation. *J Toxicol Environ Health A* **53:**615–636.

Zhang Y, Gupta A, Wang H, Zhou L, Vethanayagam RR, Unadkat JD, and Mao Q (2005) BCRP transports dipyridamole and is inhibited by calcium channel blockers. *Pharm Res* **22:**2023–2034.

Address correspondence to: C. Edwin Garner, Department of Drug Metabolism and Pharmacokinetics, AstraZeneca R&D Boston, 35 Gatehouse Road, Waltham, MA 02451. E-mail: c.edwin.garner@astrazeneca.com